

## Amine Nitrosation via NO Reduction of the Polyamine Copper(II) Complex $\text{Cu}(\text{DAC})^{2+}$

Chosu Khin, Mark D. Lim,<sup>1</sup> Kiyoshi Tsuge,<sup>2</sup> Alexei Iretskii,<sup>3</sup> Guang Wu, and Peter C. Ford\*

Department of Chemistry and Biochemistry, University of California, Santa Barbara, California 93106-9510

Received August 9, 2007

The reaction of the fluorescent macrocyclic ligand 1,8-bis(anthracen-9-ylmethyl)-1,4,8,11-tetraazacyclotetradecane with copper(II) salts leads to formation of the  $\text{Cu}(\text{DAC})^{2+}$  cation (I), which is not luminescent. However, when aqueous methanol solutions of I are allowed to react with NO, fluorescence again develops, owing to the formation of the strongly luminescent N-nitrosated ligand DAC-NO (II), which is released from the copper center. This reaction is relatively slow in neutral media, and kinetics studies show it to be first order in the concentrations of NO and base. In these contexts, it is proposed that the amine nitrosation occurs via NO attack at a coordinated amine that has been deprotonated and that this step occurs with concomitant reduction of the Cu(II) to Cu(I). DFT computations at the BP/LACVP\* level support these mechanistic arguments. It is further proposed that such nitrosation of electron-rich ligands coordinated to redox-active metal centers is a mechanistic pathway that may find greater generality in the biochemical formation of nitrosothiols and nitrosoamines.

### Introduction

There is ongoing interest in elucidating the fundamental chemistry that defines how nitric oxide (nitrogen monoxide) participates in mammalian biochemical roles such as regulation in the cardiovascular and nervous systems and cytotoxicity during immune response to pathogens.<sup>4</sup> Metal centers are known targets of NO, and a major focus of this laboratory has been to characterize the mechanistic chemistry related to the NO reactions with such sites.<sup>5</sup> One pathway is “reductive nitrosylation”, which is characterized by a reduction of an oxidizing metal center with the concomitant nitrosation of a nucleophile (eq 1)<sup>6</sup> to give nitrosated products X–NO, species that may function in NO transport<sup>7,8</sup> and signaling.<sup>9</sup> Equation 1 is also the reverse of nitrite reduction catalyzed in certain anaerobic bacteria by nitrite

reductases (NiR)<sup>10</sup> and shown to be effected by deoxyhemoglobin.<sup>11</sup>



Numerous ferriheme proteins have long been known to undergo “autoreduction” when exposed to NO in aqueous media.<sup>12</sup> Typically, these reactions proceed in two distinct steps:<sup>13</sup> the formation of a  $\text{Fe}^{\text{III}}$  nitrosyl adduct,<sup>5a</sup> followed by pH dependent reduction. The latter step can be attributed

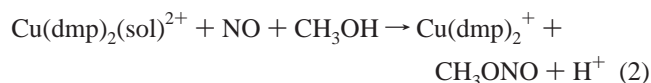
\* To whom correspondence should be addressed. E-mail: ford@chem.ucsb.edu.

- (1) (a) Current address: Department of Pharmaceutical Chemistry, University of California San Francisco, San Francisco, CA 94143-2280. (b) Taken in part from the Ph.D. Dissertation of Mark D. Lim, University of California, Santa Barbara, 2004.
- (2) Current address: Division of Chemistry, Graduate School of Science, Hokkaido University, Sapporo 060-0810, Japan.
- (3) Current address: Department of Chemistry and Environmental Sciences, Lake Superior State University, Sault Sainte Marie, MI 49783.
- (4) (a) Ignarro, L., Ed. *Nitric Oxide: Biology and Pathobiology*; Academic Press: San Diego, 2000. (b) *Nitric Oxide and Infection*; Fang, F. C., Ed.; Kluwer Academic/Plenum Publishers: New York, 1999.

- (5) (a) Hoshino, M.; Ozawa, K.; Seki, H.; Ford, P. C. *J. Am. Chem. Soc.* **1993**, *115*, 9568–9575. (b) Miranda, K. M.; Bu, X.; Lorkovic, I. M.; Ford, P. C. *Inorg. Chem.* **1997**, *36*, 4838–4848. (c) Lorkovic, I. M.; Miranda, K. M.; Lee, B.; Bernhard, S.; Schoonover, J. R.; Ford, P. C. *J. Am. Chem. Soc.* **1998**, *120*, 11674–11683. (d) Lorkovic, I. M.; Ford, P. C. *Inorg. Chem.* **1999**, *38*, 1467–1473. (e) Lorkovic, I. M.; Ford, P. C. *J. Am. Chem. Soc.* **2000**, *122*, 6516–6517. (f) Laverman, L. E.; Wanat, A.; Oszajca, J.; Stochel, G.; Ford, P. C.; van Eldik, R. *J. Am. Chem. Soc.* **2001**, *123*, 285–293. (g) Laverman, L. E.; Ford, P. C. *J. Am. Chem. Soc.* **2001**, *123*, 11614–11622. (h) Kurtikyan, T. S.; Martirosyan, G. G.; Lorkovic, I. M.; Ford, P. C. *J. Am. Chem. Soc.* **2002**, *124*, 10124–10129. (i) Lim, M. D.; Lorkovic, I. M.; Wedeking, K.; Zanella, A. W.; Works, C. F.; Massick, S. M.; Ford, P. C. *J. Am. Chem. Soc.* **2002**, *124*, 9737–9743. (j) Patterson, J. C.; Lorkovic, I. M.; Ford, P. C. *Inorg. Chem.* **2003**, *42*, 4902–4908. (k) Ford, P. C. *Pure App. Chem.* **2004**, *76*, 335–350. (l) Martirosyan, G. G.; Azizyan, A. S.; Kurtikyan, T. S.; Ford, P. C. *Chem. Commun.*, **2004**, 1488–1489. (m) Kurtikyan, T. S.; Gulyan, G. M.; Martirosyan, G. G.; Lim, M. D.; Ford, P. C. *J. Amer. Chem. Soc.*, **2005**, *127*, 6216–6224.
- (6) (a) Ford, P. C.; Fernandez, B. O.; Lim, M. D. *Chem. Rev.* **2005**, *105*, 2439–2455. (b) Gwost, D.; Caulton, K. G. *Inorg. Chem.* **1973**, *12*, 2095.

to hydroxide attack on the activated nitrosonium group ( $\text{Fe}^{\text{III}}(\text{NO}) \leftrightarrow \text{Fe}^{\text{II}}(\text{NO}^+)$ ) to form nitrite ion plus the ferrous protein.<sup>13</sup> The latter readily reacts with excess NO to form very stable ferroheme nitrosyl complexes  $\text{Fe}^{\text{II}}(\text{NO})$ . The NO reductions of ferriheme proteins and of water-soluble iron(III) porphyrinato models are subject to catalysis by nitrite ion itself.<sup>14</sup>

Although not as extensively studied as the ferriheme systems, copper(II) models and proteins are also reduced by NO.<sup>15–18</sup> An earlier quantitative study from this laboratory described the NO reduction of  $\text{Cu}(\text{dmp})_2(\text{sol})^{2+}$  ( $\text{dmp} = 2,9$ -dimethyl-1,10-phenanthroline,  $\text{sol} = \text{solvent}$ ) (eq 2) and related derivatives.<sup>16</sup> This reaction is accompanied by nitrosation of the solvent (forming  $\text{MeO}-\text{NO}$  in methanol and  $\text{NO}_2^-$  in water).



X–NO products such as *N*-nitrosoamines and *S*-nitrosothiols are broadly distributed in mammalian tissue and

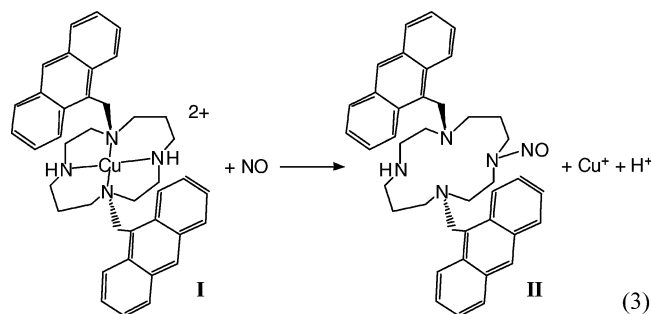
fluids and may serve as bioavailable reservoirs of NO and in biological signaling.<sup>9,19</sup> While there are several pathways for generating these species, Cu(II) has been shown to promote the nitrosation of thiols such as bovine serum albumin and glutathione (GSH).<sup>20</sup> Similar reactions are promoted by the copper protein ceruloplasmin found in vertebrate blood plasma.<sup>21</sup>

In 2004,<sup>22</sup> we reported the reaction of NO with the copper(II) complex  $\text{Cu}(\text{DAC})^{2+}$  (**I**), where DAC is the *N*-derivatized cyclam 1,8-bis(anthracen-9-ylmethyl)-1,4,8,11-tetraazacyclotetradecane. The initial goal was to develop a sensor based on a luminescent chromophore quenched by the low-lying ligand field states of the Cu(II) center. The expectation was that the system would become emissive upon reaction with NO to give a diamagnetic adduct ( $\text{Cu}^{\text{I}}(\text{NO}) \leftrightarrow \text{Cu}^{\text{I}}(\text{NO}^+)$ ) or Cu(I) reduction product, as we had demonstrated for  $\text{Cu}(\text{dmp})_2(\text{sol})^{2+}$ .<sup>17</sup> With a similar motive, we had prepared Cu(II) complexes of bis(2-(3,5-dimethyl-1-pyrazolyl)ethyl)amine (pza) with appended Ru(II) and Re(I) luminophores,<sup>23</sup> although the pza complexes of Cu(I) and Cu(II) proved too labile to serve as practical sensors. Consistent with the above expectation, a luminescent product was indeed formed upon the interaction of NO with solutions of **I**,<sup>22</sup> but the reaction was too slow under near-neutral conditions to serve as a real-time sensor.

It should be noted, however, that a similar strategy has been implemented for copper-based NO sensors designed by Lim, Lippard, and co-workers.<sup>24</sup> In those cases, the cupric complexes utilized were  $\text{Cu}(\text{Ds-AMP})_2$  and  $\text{Cu}(\text{Ds-en})_2$ , where DS-en and DS-AMP are the conjugate bases of the fluorophores dansyl ethylenediamine and dansyl aminomethylpyridine, respectively. A more recent report by Xing et al.<sup>25</sup> extends this approach.

The unexpected result from the reaction of  $\text{Cu}(\text{DAC})^{2+}$  with NO was the nitrosation of coordinated amine concomitant with copper reduction to Cu(I) leading to formation of the *N*-nitrosoamine compound **II** when complex **I** was exposed to NO (eq 3,  $\text{R} = \text{anthracenyl}$ ).<sup>22</sup> This demonstrated a previously unrecognized pathway for the metal-promoted *N*-nitrosation of a coordinated ligand, which has now been observed for the reactions of  $\text{Cu}(\text{Ds-AMP})_2$  and  $\text{Cu}(\text{Ds-en})_2$  with NO which gave *N*-nitrosation of the DS-en and DS-AMP ligands.<sup>24</sup> In the present report, we describe quantitative

- (7) (a) Gow, A. J.; Luchsinger, B. P.; Pawloski, J. R.; Singel, D. J.; Stampler, J. S. *Proc. Nat. Acad. Sci. U.S.A.* **1999**, *96*, 9027. (b) Luchsinger, B. P.; Rich, E. N.; Gow, A. J.; Williams, E. M.; Stampler, J. S.; Singel, D. J. *Proc. Nat. Acad. Sci. U.S.A.* **2003**, *100*, 461.
- (8) see also (a) Gladwin, M. T.; Lancaster, J. R., Jr.; Freeman, B. A.; Schechter, A. N. *Nature Med.* **2003**, *9*, 496. (b) Han, T. H.; Fukuto, J. M.; Liao, J. C. *NO Bio. Chem.* **2004**, *10*, 74.
- (9) (a) Feelisch, M. S.; Rassaf, T.; Manimneh, S.; Singh, N.; Byran, N. S.; Jourd'Heuil, D.; Kelm, M. *FASEB J.* **2002**, *16*, 1775. (b) Bryan, N. S.; Rassaf, T.; Maloney, R. E.; Rodriguez, C. M.; Saijo, F.; Rodriguez, J. R.; Feelisch, M. *Proc. Nat. Acad. Sci., U.S.A.* **2004**, *101*, 4308. (c) Rassaf, T.; Feelisch, M.; Kelm, M. *Free Rad. Bio. Med.* **2004**, *36*, 413–422. (d) Bryan, N. S.; Fernandez, B. O.; Bauer, S. M.; Garcia-Saura, M. F.; Milsom, Alexandra B.; Rassaf, T.; Maloney, R. E.; Bharti, A.; Rodriguez, J.; Feelisch, M. *Nat. Chem. Biol.* **2005**, *1*, 290–297.
- (10) Wasser, I. M.; de Vries, S.; Moenne-Loccoz, P.; Schroeder, I.; Karlin, K. D. *Chem. Rev.* **2002**, *102*, 1201, and references therein.
- (11) (a) Doyle, M. P.; LePoire, D. M.; Pickering, R. A. *J. Biol. Chem.* **1981**, *256*, 12399–404. (b) Huang, K. T.; Keszler, A.; Patel, N.; Patel, Rakesh, P.; Gladwin, M. T.; Kim-Shapiro, D. B.; Hogg, N. *J. Biol. Chem.* **2005**, *280*, 31126–31131. (c) Huang, Z.; Shiva, S.; Kim-Shapiro, D. B.; Patel, R. P.; Ringwood, L. A.; Irby, C. E.; Huang, K. T.; Ho, C.; Hogg, N.; Schechter, A. N.; Gladwin, M. T. *J. Clin. Investig.* **2005**, *115*, 2099–2107. (d) Gladwin, M. T.; et al. *Nat. Chem. Biol.* **2005**, *1*, 308–314.
- (12) (a) Chien, J. C. W. *J. Am. Chem. Soc.* **1969**, *91*, 2166–2168. (b) Wayland, B. B.; Olson, L. W. *J. Am. Chem. Soc.* **1974**, *96*, 6037–6041.
- (13) Hoshino, M.; Maeda, M.; Konishi, R.; Seki, H.; Ford, P. C. *J. Am. Chem. Soc.* **1996**, *118*, 5702–5707.
- (14) (a) Fernandez, B. O.; Ford, P. C. *J. Am. Chem. Soc.* **2003**, *125*, 10510–10511. (b) Fernandez, B. O.; Lorkovic, I. M.; Ford, P. C. *Inorg. Chem.* **2004**, *43*, 5393–5402.
- (15) (a) Martin, C. T.; Morse, R. H.; Kanne, R. M.; Gray, H. B.; Malmstrom, B. G.; Chan, S. I. *Biochem.* **1981**, *20*, 5147. (b) Gorren, A. C. F.; de Boer, E.; Wever, R. *Biochem. Biophys. Acta* **1987**, *916*, 38–47. (c) Cooper, C. E.; Torres, J.; Sharpe, M. A.; Wilson, M. T. *FEBS Lett.* **1997**, *414*, 281. (d) Torres, J.; Cooper, C. E.; Wilson, M. T. *J. Biol. Chem.* **1998**, *273*, 8756. (e) Torres, J.; Svistunenko, D.; Karlsson, B.; Cooper, C. E.; Wilson, M. T. *J. Am. Chem. Soc.* **2002**, *124*, 963–967.
- (16) (a) Tran, D.; Skelton, B. W.; White, A. H.; Laverman, L. E.; Ford, P. C. *Inorg. Chem.* **1998**, *37*, 2505–2511. (b) Tran, D.; Ford, P. C. *Inorg. Chem.* **1996**, *35*, 2411–2412. (c) Lim, M. D.; Capps, K. B.; Karpishin, T. B.; Ford, P. C. *Nitric Oxide, Biol. Chem.* **2005**, *12*, 244–251.
- (17) (a) Brown, G. C. *Biochim. Biophys. Acta* **2001**, *1504*, 46–57. (b) Torres, J.; Sharpe, M. A.; Rosquist, A.; Cooper, C. E.; Wilson, M. T. *FEBS Lett.* **2000**, *475*, 263–266.
- (18) Wijma, H. J.; Canters, G. W.; de Vries, S.; Verbeet, M. P. *Biochem.* **2004**, *43*, 10467–10474.
- (19) Gladwin, M. T.; et al. *Nat. Med.* **2003**, *9*, 1498–1505.
- (20) (a) Stubauer, G.; Giuffre, A.; Sartì, P. *J. Biol. Chem.* **1999**, *274*, 28128–28133. (b) Inoue, K.; Akaike, T.; Miyamoto, Y.; Okamoto, T.; Sawa, T.; Otagiri, M.; Suzuki, S.; Yoshimura, T.; Maeda, H. *J. Biol. Chem.* **1999**, *274*, 27069–27075.
- (21) Shiva, S.; Wang, X.; Ringwood, L. A.; Xu, X.; Yuditskaya, S.; Annavajjhala, V.; Miyajima, H.; Hogg, N.; Harris, Z. L.; Gladwin, M. T. *Nat. Chem. Biol.* **2006**, *2*, 486–493.
- (22) Tsuge, K.; DeRosa, F.; Lim, M. D.; Ford, P. C. *J. Am. Chem. Soc.* **2004**, *126*, 6564–6565.
- (23) Riklin, M.; Tran, D.; Bu, X.; Laverman, L. E.; Ford, P. C. *J. Chem. Soc., Dalton Trans* **2001**, 1813–1819.
- (24) (a) Lim, M. H.; Lippard, S. J. *J. Am. Chem. Soc.* **2005**, *127*, 12170–12171. (b) Lim, M. H.; Xu, D.; Lippard, S. J. *Nat. Chem. Biol.* **2006**, *2*, 375–380. (c) Lim, M. H.; Wong, B. A.; Pitcock, W. H., Jr.; Mokshagundam, D.; Baik, M.-H.; Lippard, S. J. *J. Am. Chem. Soc.* **2006**, *128*, 14364–14373. (d) Smith, R. C.; Tennyson, A. G.; Won, A. C.; Lippard, S. *Inorg. Chem.* **2006**, *45*, 9367–9373.
- (25) Xing, C.; Yu, M.; Wang, S.; Shi, Z.; Li, Y.; Zhu, D. *Macromol. Rapid Commun.* **2007**, *28*, 241–245.



experimental and computational studies designed to elucidate the reaction of Cu(DAC)<sup>2+</sup> with NO and discuss the potential extension of this mechanism to nitrosations of other nucleophiles coordinated to redox-active metals.<sup>25</sup> We will also expand upon experimental observations reported in our initial communication describing this reaction.<sup>22</sup>

## Experimental Section

**Materials.** Solutions for kinetics studies were prepared under argon with purified solvents using standard Schlenk line techniques or an argon-filled glovebox. Solvents (Fischer) were distilled and deoxygenated following standard procedures. Aqueous solutions were prepared with doubly distilled water and deoxygenated by boiling under reduced pressure. CuBr<sub>2</sub> (Strem Chemicals) and AgPF<sub>6</sub> (Aldrich) were used as received. NO (Aire Liquide) was purified by passage through an Ascarite II column (Thomas Scientific), and solutions of known [NO] were prepared using transfer techniques on a greaseless vacuum line as described elsewhere.<sup>5i,26</sup> Isotopically labeled <sup>15</sup>N<sup>18</sup>O was purchased from Cisotec, Inc.

The ligand DAC was prepared according to a published procedure.<sup>27</sup>

**Syntheses. [Cu(DAC)]Br<sub>2</sub>·2H<sub>2</sub>O.** A methanol solution (2 mL) of CuBr<sub>2</sub> (13 mg, 5.8 × 10<sup>-5</sup> mol) was added to a DMF suspension (8 mL) of DAC (20 mg, 3.5 × 10<sup>-5</sup> mol). After sonication, the resultant green solution was concentrated to a volume of ~2 mL. The deposited orange crystals were collected by filtration and washed with MeOH. Yield: 24 mg, 79%. UV-vis (in 1:1 DMF/MeOH v/v) (λ<sub>max</sub> in nm (ε in M<sup>-1</sup> cm<sup>-1</sup>)): 338 (8.69 × 10<sup>3</sup>), 356 (1.32 × 10<sup>4</sup>), 374 (1.82 × 10<sup>4</sup>), 394 (1.60 × 10<sup>4</sup>), 356 (2.66 × 10<sup>2</sup>). Anal. Calcd for C<sub>42</sub>H<sub>52</sub>Br<sub>2</sub>CuN<sub>4</sub>O<sub>2</sub>: C, 58.10; H, 6.04; N, 6.45. Found: C, 58.00; H, 5.76; N, 6.84.

[Cu(DAC)](PF<sub>6</sub>)<sub>2</sub> was prepared from the bromide salt by anion exchange with AgPF<sub>6</sub>. A solution of [Cu(DAC)]Br<sub>2</sub>·2H<sub>2</sub>O (22.3 mg, 2.6 × 10<sup>-5</sup> mol) was prepared in 1:1 DMF/MeOH, and AgPF<sub>6</sub> (14.2 mg, 5.6 × 10<sup>-5</sup> mol) was added, leading to the precipitation of AgBr, which was removed by filtration. The solvent was removed by evaporation to give an orange crystalline material that was then recrystallized from CH<sub>3</sub>CN/Et<sub>2</sub>O. Yield 19.8 mg, 83%. Anal. Calcd for C<sub>40</sub>H<sub>44</sub>CuF<sub>12</sub>N<sub>4</sub>P<sub>2</sub>: C, 51.42; H, 4.75; N, 6.00. Found: C, 51.65; H, 4.67; N, 6.02.

**Emission Measurements.** Emission and excitation spectra were recorded utilizing a SPEX Fluorolog 2 spectrofluorimeter equipped with a Hamamatsu R928-A water-cooled PMT configured for photon counting and interfaced with a computer running Spex DM3000f software. Emission spectra were corrected for PMT

response and for lamp intensity variation by the ratio method with a Rhodamine-6G reference.

**Electrochemical Measurements.** Cyclic voltammetry measurements were made using a BAS 100A electrochemical analyzer with an Ag/AgCl reference electrode, a glassy carbon working electrode, and a Pt wire counter electrode. Tetrabutylammonium perchlorate (TBAP) was recrystallized from methanol and stored in the glovebox prior to its use as an electrolyte. Solvents were distilled and stored over molecular sieves. Ferrocene (Fc) was recrystallized and used as an internal standard for all measurements. All sample solutions were deoxygenated by entraining with argon for 15 min while vigorously stirring. Half-wave potentials were measured as the average of the anodic and cathodic peak potentials.

**Kinetic Measurements.** The [Cu(DAC)]X<sub>2</sub> salts are only sparingly soluble in water, so rates of the NO reaction with I were monitored in an 8:2 (v/v) methanol/water solvent. Before adding the methanol, the base concentration in aqueous component was adjusted with NaOH stock solution or stabilized near pH 7 using a NaH<sub>2</sub>PO<sub>4</sub>/Na<sub>2</sub>HPO<sub>4</sub> buffer (μ = 0.15 M). Solutions of [Cu(DAC)]X<sub>2</sub> were prepared using syringe techniques in an argon-filled glovebox.

The slower reactions were initiated by injecting solutions of I from a gastight syringe into a NO-filled cell using custom-made cuvettes permanently fused to a flask equipped with a high-vacuum stopcock and a cold finger. This procedure allowed for the anaerobic preparation of solutions containing a known [NO] for each individual kinetics experiment. Although such solutions were prepared by procedures designed to minimize contamination with nitrite and other higher oxides,<sup>26</sup> the most likely source of uncertainty in the kinetics data is likely to be the NO concentrations in these solutions. Changes in the optical spectra were monitored at regular intervals using the kinetics program on an HP 8452A diode array spectrophotometer. Solutions were agitated periodically to ensure the continuous equilibration between the gas and solution phases and to maintain pseudo-first-order conditions (excess [NO]). Faster reactions (at the higher pH values) were monitored by following absorbance changes at 393 nm (ππ\* anthracene band) using an Applied Photophysics SX-18MV stopped-flow spectrophotometer. All reactions were thermostated at 298 K.

No significant differences were observed in the kinetics of the NO reactions with the different salts (bromide, hexafluorophosphate, or perchlorate) of I. This is likely due to the low concentrations of I used in these experiments (typically about 0.1 mM).

**NMR and IR Measurements.** The reactions were also monitored by proton NMR on a Varian 400 or 500 MHz NMR spectrometer in 10:1 CD<sub>3</sub>CN/CD<sub>3</sub>OD (Cambridge Isotopes Laboratories) in an anaerobic NMR tube sealed by a Teflon stopcock (C. Young). Infrared spectra with 1 cm<sup>-1</sup> resolution were recorded with a research series FT Mattson FTIR spectrophotometer from 400 to 4000 cm<sup>-1</sup>.

**Structure Determination.** The structure of the cupric cation I determined by X-ray crystallography of the salt [Cu(DAC)](PF<sub>6</sub>)<sub>2</sub> is shown in Figure 1. The crystal structure data and the cell packing diagram are presented in the Supporting Information (Tables S1a–1f and Figure S1). A red crystal of approximate dimensions 0.25 × 0.1 × 0.06 mm<sup>3</sup> was mounted on a glass fiber and transferred to a Bruker CCD platform diffractometer. The SMART program<sup>28</sup> was used to determine the unit cell parameters and data collection (20 s/frame, 0.3 deg/frame for a sphere of diffraction data) at room temperature (293 K). The raw frame data were processed using

(26) Lim, M. D.; Lorkovic, I. M.; Ford, P. C. *Methods Enzymol.* **2005**, *396*, Part E, 3–17.

(27) DeRosa, F.; Bu, X.; Ford, P. C. *Inorg. Chem.* **2003**, *42*, 4171–4178.

(28) *SMART Software Users Guide, Ver 5.1*; Bruker Analytical X-ray Systems, Inc: Madison, WI, 1999.

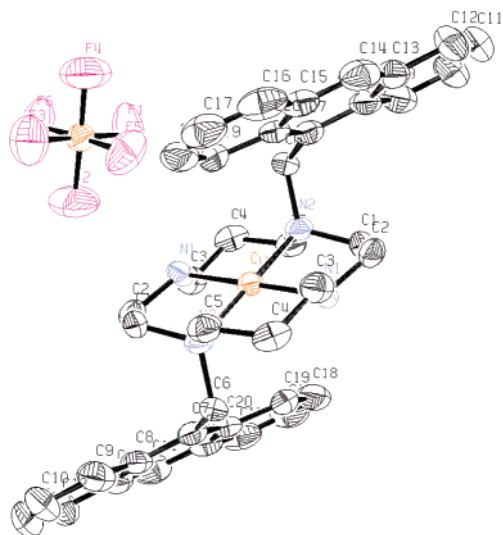


**Figure 1.** ORTEP diagram of **I** determined for a crystal of  $[\text{Cu}(\text{DAC})](\text{PF}_6)_2$  showing one of the  $\text{PF}_6^-$  counterions. Thermal ellipsoids are shown at 50% probability.

the SAINT program,<sup>29</sup> and the absorption correction was applied using the SADABS program.<sup>30</sup> Subsequent calculations were carried out using the SHELXTL program.<sup>31</sup> The  $P2(1)/a$  space group was determined from the system absence of the reflection intensities. The structure was solved by direct methods and refined on  $F^2$  by full-matrix least-squares techniques. Hydrogen atoms were theoretically added. At convergence,  $wR2 = 0.1649$  and  $\text{GOF} = 1.116$  for 272 variables refined against 2716 reflections, while  $R1 = 0.0664$  for 1704 reflections with  $I > 2\sigma(I)$ .

The X-ray crystal structure of the perchlorate salt,  $[\text{Cu}(\text{DAC})](\text{ClO}_4)_2$ , was also determined, and this is described in the Supporting Information (Figures S2 and S3; Tables S2a–S2f).

**Computations.** DFT calculations were performed at the BP/LACVP\* theory level. The choice of the BP model was based on the fact that other DFT models (BLYP, B3LYP) lead to larger errors in bond lengths for copper complexes.<sup>32</sup> The geometry of  $[\text{Cu}(\text{DAC})(\text{OH})]^+$  was first optimized using the Titan software suite (Wavefunction, Inc.), and then the energy was recalculated using Spartan'04 software (Wavefunction, Inc.) due to the difficulties in self-consistent field (SCF) convergence within Spartan'04. All other compounds were optimized within Spartan'04. The optimization procedure began with conformation analysis (MMFF) from which the geometry of the lowest energy conformer was optimized without use of symmetry constraints.

## Results and Discussion

As noted in the Introduction, an incentive for preparing **I** was to probe its luminescence response to nitric oxide, since the  $d^9$  Cu(II) of **I** was expected to quench the  $\pi\pi^*$  fluorescence from the anthracenyl groups (free DAC does indeed show strong fluorescence). As predicted, solutions of **I** displayed virtually no emission while exposure of ambient temperature solutions of **I** to NO resulted in strongly

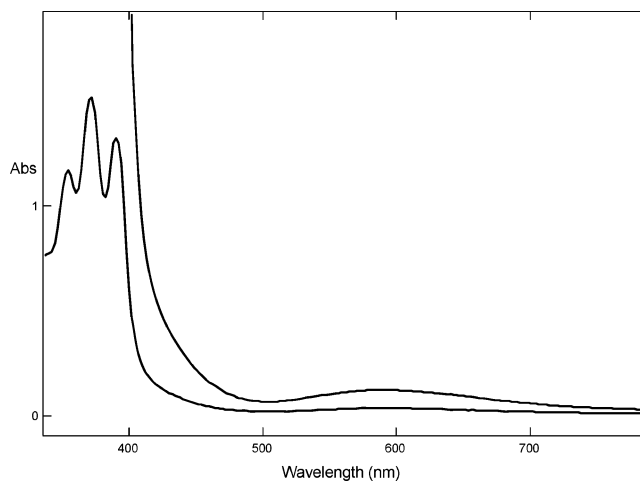


**Figure 2.** Electronic spectrum of  $[\text{Cu}(\text{DAC})]\text{Br}_2$  (0.6 mM) in 1:1 (v/v) dimethylformamide/methanol solution. The vertical scale of the spectrum at longer wavelength has been expanded to show the weak visible range ligand field absorption.

enhanced fluorescence from the pendant chromophores. However, the developing emission and corresponding changes in the solution absorption spectra occurred over a period of minutes, much slower than would be anticipated for simple NO coordination to a Cu(II) center. Furthermore, examination of the products revealed the unexpected nitrosation of the macrocyclic ligand concomitant with reduction of Cu(II) to Cu(I) (eq 3).<sup>22</sup> The studies reported here probe the mechanism of this reaction.

**Characterization of I.** The structure of **I** determined by single-crystal X-ray diffraction studies of  $[\text{Cu}(\text{DAC})](\text{PF}_6)_2$  (Figure 1) shows the copper(II) to have nearly square planar coordination with the four nitrogens of the macrocyclic tetraamine ligand. The Cu–N bonds to the tertiary nitrogens bearing the anthracenyl groups are slightly longer (2.058(5) Å) than those to the secondary amine nitrogens (1.989(5) Å). The pendant anthracenyl chromophores are positioned above and below the  $\text{CuN}_4$  square plane.

The X-ray crystal structure data for the perchlorate salt,  $[\text{Cu}(\text{DAC})](\text{ClO}_4)_2$ , show that there are no significant structural differences between the  $\text{Cu}(\text{DAC})^{2+}$  cations in these two salts.

The electronic spectrum of **I** in dimethylformamide/methanol (1:1) displays broad ligand field (d–d) band at  $\lambda_{\text{max}} = 566 \text{ nm}$  ( $\epsilon = 266 \text{ M}^{-1} \text{ s}^{-1}$ ) (Figure 2), as well as the strong  $\pi\text{--}\pi^*$  absorption bands at 350–400 nm ( $\epsilon \approx 10^4 \text{ M}^{-1} \text{ s}^{-1}$ ) characteristic of the pendant anthracenyl groups.<sup>22</sup>

Cyclic voltammetry of  $[\text{Cu}(\text{DAC})]\text{Br}_2$  in DMF/MeOH mixed solvent (1:1 v/v) gave a single reversible reduction from which was determined a reduction potential of  $-0.61 \text{ V}$  vs  $\text{Fc}^+/\text{Fc}$ , determined in the same solution.

**Emission Measurements.** The emission spectrum ( $\lambda_{\text{ex}} = 350 \text{ nm}$ ) of  $[\text{Cu}(\text{DAC})](\text{PF}_6)_2$  was examined at ambient temperature in methanol and MeOH/H<sub>2</sub>O solutions and at 77 K in MeOH/EtOH 1:4 frozen glasses. Under neither circumstance was any emission from these solutions apparent. The absence of the anthracene-centered fluorescence, which is strong for the free DAC ligand under these conditions, is consistent with expectation that luminescence

(29) *S SAINT Software Users Guide, Ver. 5.1*; Bruker Analytical X-ray Systems: Madison, WI, 1999.

(30) Sheldrick, G. M. *SADABS, Ver. 2.05*; Bruker Analytical Systems, Inc.: Madison, WI, 2001.

(31) Sheldrick, G. M. *SHELXTL, Ver. 6.12*; Bruker Analytical X-ray Systems: Madison, WI, 2001.

(32) Hehre, W. J. *A Guide to Molecular Mechanics and Quantum Chemical Calculations*; Wavefunction, Inc.: Irvine, CA, 2003; p 796.

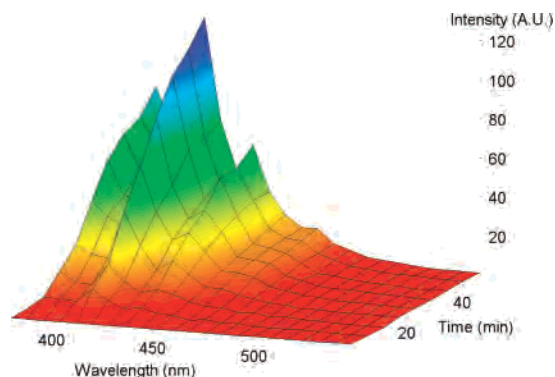


**Figure 3.** Temporal emission spectrum of a 298 K solution of [Cu(DAC)]-(PF<sub>6</sub>)<sub>2</sub> ( $1.7 \times 10^{-5}$  M) in 10:1 (v/v) MeOH/H<sub>2</sub>O following the addition of NO (12 mM). The spectrum ( $\lambda_{\text{exc}} = 350$  nm) was recorded every 3 min for 45 min.

from the pendant anthracene chromophores of **I** would be quenched by energy transfer to low-lying ligand field states of the d<sup>9</sup> copper(II) center. When ambient-temperature solutions of **I** were exposed to NO, a structured emission in the 380–480 nm range characteristic of anthracene luminophores appeared. Thus, the system is an NO sensor. However, as is illustrated by the time-dependent spectrum in Figure 3, the rise of the fluorescence after the addition of NO occurred slowly by a pH-dependent pathway over a period of many minutes. Furthermore, the transformation was irreversible; removal of NO from the solution by evacuating the flask after the reaction did not affect the emission spectrum. Thus, the spectral changes are not the result of the reversible formation of NO adduct, since these would be expected to be quite fast given the lability generally seen for cupric ion ligand substitution reactions. Instead, as demonstrated below, the chemical transformations are more complex.

**Products of the Reaction of I with NO.** As we have reported,<sup>22</sup> NO addition to [Cu(DAC)]Br<sub>2</sub> solutions in deaerated methanol or acetonitrile leads to slow bleaching of the initially orange color attributed to the ligand field absorption band centered at 566 nm. Correspondingly, the fluorescence spectrum (Figure 3) is characterized by the appearance of an anthracene-like luminescence on the same time frame (minutes) as the changes in the absorption spectrum (see below). The <sup>1</sup>H NMR spectra of analogous solutions of **I** also demonstrated marked changes upon addition of NO. This is illustrated by the spectra of **I** in CD<sub>3</sub>-CN. Prior to NO addition, this displayed only the broad resonances expected for a paramagnetic complex, but after reaction with excess NO, the <sup>1</sup>H NMR spectra showed the sharp resonances for a diamagnetic organic ligand with multiple resonances in the range of 7.4–8.5 ppm characteristic of the anthracenyl moiety, 2.2–4.2 ppm due to methylene protons in the ring, and 4.4–4.7 ppm for the anthracenylmethyl protons. While such changes would be consistent with the reduction of Cu(II) to Cu(I), an alternative explanation might be the simple, reversible formation of a diamagnetic nitrosyl complex Cu(DAC)(NO)<sup>2+</sup>. However, since these NMR changes were not reversed by vacuum removal of the NO in the solution, the latter scenario is unlikely. In support

of the former pathway, electrochemical analysis of product solutions indicated the presence of an oxidizable species having the same potential (0.4 V vs Ag/AgCl) as found in solutions prepared by adding CuBr to analogous solvent mixtures (1:1 DMF/MeOH). On these bases, we concluded that the reaction of NO with **I** leads to the irreversible reduction of Cu(II) to Cu(I).

The addition of diethyl ether to a concentrated reaction solution forced a precipitation of an organic product that was identified as the *N*-nitrosated cyclam ligand DAC-NO (**II**). The positive ion ESI-mass spectrum of its solution displayed a large peak ( $M^+$ ) at 610 ( $m/z$ ) and a small one at 580. The first corresponds to **II** (mass = 609 au) protonated to give the 610  $m/z$  cation ( $M^+ = \{\text{DAC} - \text{NO} + \text{H}^+\}^+$ ) in the ESI-MS<sup>+</sup> experiment. The analogous experiment using isotopically labeled <sup>15</sup>N<sup>18</sup>O gave an  $M^+$  at 613 ( $m/z$ ), corresponding to  $\{\text{DAC} - {}^{15}\text{N}^{18}\text{O} + \text{H}^+\}^+$ . In contrast, the ESI-MS<sup>+</sup> spectrum of free DAC gave a parent peak of 581 ( $m/z$ ) corresponding to  $M^+ = \{\text{DAC} + \text{H}^+\}^+$ ; therefore, the small 580  $m/z$  cation found in the product spectrum would appear to be the result of NO loss from **II** and protonation to give the radical cation  $\{\text{II} - \text{NO} + \text{H}^+\}^+$ . No peaks at  $m/z$  ratios corresponding to copper complexes of DAC or its derivatives were found in the ESI-MS<sup>+</sup> analysis of the reaction products.

The <sup>1</sup>H NMR spectrum of **II** in CD<sub>3</sub>CN is also consistent with the assignment of this material as the *N*-nitrosated cyclam ligand DAC-NO that is present in two isomeric forms due to a high rotational barrier of 23–29 kcal/mol about the N–N bond as it was found for other aliphatic cyclic nitrosamine systems.<sup>34</sup> The <sup>1</sup>H-COSY analysis gave 20 proton signals in the aliphatic region that could all be assigned to the two isomers of **II**. These include resonances at 4.16, 3.88, 3.47, and 3.39 ppm in the range for *cis* and *trans*  $\alpha$ -protons for aliphatic nitrosoamines. For the anthracenylmethyl groups, four singlets are attributed to the methylene protons (4.44, 4.56, 4.69, and 4.72 ppm) and four sets of signals for anthracenyl protons (7.4–8.5 ppm), again consistent with the formation of two isomers. The presence of two conformers/isomers of **II** in roughly equal proportions has been confirmed by mass spectrometric–ion mobility experiments.<sup>35</sup> (These spectra are described in more detail in the Supporting Information).

The IR spectrum of **II**, recorded in KBr pellets, shows a strong band at 1452 cm<sup>-1</sup>, which was not present in the spectrum of DAC and corresponds to  $\nu_{\text{NO}}$  of a free nitrosamine.<sup>33</sup> This band is shifted to 1377 cm<sup>-1</sup> upon substitution of <sup>15</sup>N<sup>18</sup>O for standard nitric oxide, which is in a good agreement with the expected value for NN=O vibrational frequency after the isotopic substitution. If instead of isolating

- (33) (a) Lee, J.; Chen, L.; West, A. H.; Richter-Addo, G. B. *Chem. Rev.* **2002**, *102*, 1019–1065. (b) Chen, L.; Yi, G. B.; Wang, L. S.; Dharmawardana, U. R.; Dart, A. C.; Khan, M. A.; Richter-Aldo, G. B. *Inorg. Chem.* **1998**, *37*, 4677–4688.  
 (34) Cooney, J. D.; Brownstein, S. K.; Simon, J. W. *Can. J. Chem.* **1974**, *52*, 3028–3036.  
 (35) Baker, E. S.; Bushnell, J. E.; Weckler, S.; Lim, M. D.; Manard, M. J.; Dupuis, N. F.; Ford, P. C.; Bowers, M. T. *J. Am. Chem. Soc.* **2005**, *127*, 18222–18228.

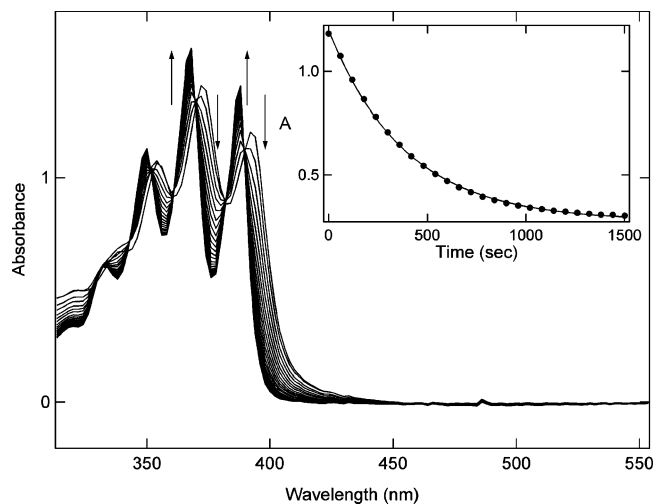


**Figure 4.** Changes in the UV–vis spectrum of  $[\text{Cu}(\text{DAC})]\text{Br}_2$  dissolved in 80:20 methanol/buffered aqueous solution at 298 K upon the introduction of NO. Spectra were recorded every 60 s for 1500 s. Inset: The single-exponential fit (solid line) to the temporal absorbance (dots) at 393 nm.

**II**, one takes the IR spectrum of the solid residue that resulted upon removal of a solvent after the reaction of **I** with NO, a strong band at  $1270\text{ cm}^{-1}$  consistent with coordinated nitrosamine is evident.<sup>33b</sup> When the same experiment was conducted with  $^{15}\text{N}^{18}\text{O}$ , the only change in the spectra was the shift of that band to  $1217\text{ cm}^{-1}$ . However, the spectrum of this mixture, redissolved in  $\text{CD}_3\text{CN}$  solution, shows only an IR band at  $1430\text{ cm}^{-1}$  consistent with the expected  $\nu_{\text{NO}}$  of a free nitrosamine. It is likely that in solution any interaction of Cu(I) center with nitrosamine in such solutions is weak.

**Kinetics Studies of the NO Reaction with  $\text{Cu}(\text{DAC})^{2+}$ .** Exposing solutions of **I** ( $\text{Br}^-$  or  $\text{PF}_6^-$  salts) to NO in various solvents leads to changes in their electronic spectra, the temporal behavior of which are strongly dependent on the conditions. For example, in unbuffered MeOH/ $\text{H}_2\text{O}$  solution, the slow spectroscopic changes appeared to display an induction period. These changes were slowed by added acid but were accelerated by added base. The putative induction period under neutral conditions was no longer apparent when the solutions were buffered, so this behavior likely results from shifts in the effective pH during the course of the reaction.

Figure 4 illustrates the temporal changes in the absorption spectrum over a period of 1500 s after introduction of NO (0.7 atm) to a 298 K solution of  $[\text{Cu}(\text{DAC})]\text{Br}_2$  ( $\sim 0.09\text{ mM}$ ). The solvent in this case was a 80:20 (v/v) mixture of methanol and aqueous phosphate buffer (0.10 M, pH 7.4 in water). The NO solubility under these conditions was estimated as  $10.7\text{ mM atm}^{-1}$  based on NO solubilities in water ( $1.8\text{ mM atm}^{-1}$ ) and in MeOH ( $14\text{ mM atm}^{-1}$ ) and the solvent ratio. During this relatively slow reaction, NO equilibration between gas and liquid phase was maintained by periodic agitation of the solution. These spectral changes display a number of isosbestic points, implying that a single spectrally significant product is formed or, alternatively, that multiple products are formed in a constant ratio. When the absorbance at a single wavelength (393 nm) was plotted

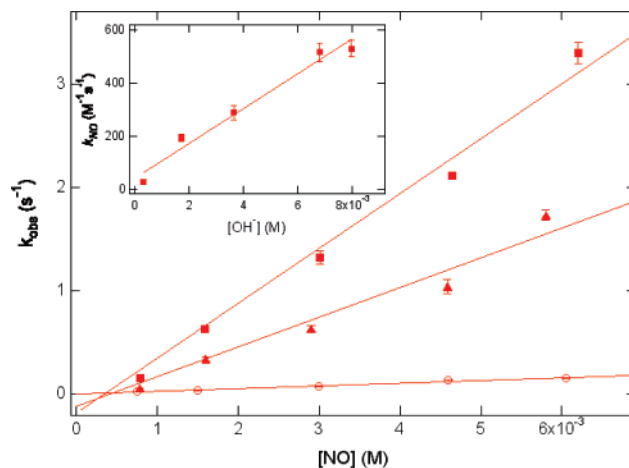


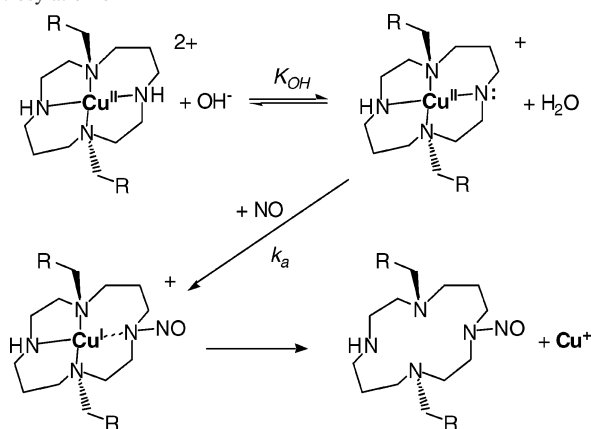
**Figure 5.** Plots of  $k_{\text{obs}}$  for eq 10 vs  $[\text{NO}]$  at different base concentrations demonstrating the linear dependence on  $[\text{NO}]$  under each set of conditions and the dependence of the resulting  $k_{\text{NO}}$  values on base concentration. Circles:  $[\text{NaOH}] = 3.4 \times 10^{-4}\text{ M}$  ( $k_{\text{NO}} = 27 \pm 2\text{ M}^{-1}\text{ s}^{-1}$ ); triangles:  $3.6 \times 10^{-3}\text{ M}$  ( $k_{\text{NO}} = 290 \pm 30\text{ M}^{-1}\text{ s}^{-1}$ ); squares:  $8.0 \times 10^{-3}\text{ M}$  ( $k_{\text{NO}} = 530 \pm 30\text{ M}^{-1}\text{ s}^{-1}$ ). Inset: plot of  $k_{\text{NO}}$  vs  $[\text{NaOH}]$  ( $k_3 = (6.5 \pm 0.6) \times 10^4\text{ M}^{-2}\text{ s}^{-1}$ ). Conditions:  $\text{Cu}(\text{DAC})\text{Br}_2$  in 80:20 MeOH/water at 298 K.

versus time, a simple decay was observed with no induction period (see Figure 4 inset). Such data fit well to exponential decays from which the observed rate constants,  $k_{\text{obs}}$ , were extracted.

The dependence of the reaction rates on the NO concentration was investigated under conditions defined by varying the nitric oxide partial pressure,  $P_{\text{NO}}$ , while holding the other variables (solvent, ionic strength, base concentration, temperature) constant. The resulting  $k_{\text{obs}}$  values gave a linear plot vs  $[\text{NO}]$ , the slope of which was the second-order rate constant,  $k_{\text{NO}}$ , for a specific base concentration. Accordingly, the  $k_{\text{NO}}$  values were determined in the 8:2 MeOH/water solvent mixture for five different concentrations of base (added as NaOH) from the slopes of  $k_{\text{obs}}$  plots vs  $[\text{NO}]$  as illustrated in Figure 5 for three such base concentrations. The  $k_{\text{obs}}$  values for the higher base concentrations were determined using a stopped-flow spectrophotometer at 298 K, while the slower rates at lesser values of  $[\text{OH}^-]$  were recorded using a conventional diode array spectrophotometer. A plot of  $k_{\text{NO}}$  vs  $[\text{OH}^-]$  is linear (Figure 5, inset) with an  $(x,y)$  intercept, within experimental uncertainty of zero. The slope of this plot  $(6.5 \pm 0.6) \times 10^4\text{ M}^{-2}\text{ s}^{-1}$  would be the rate constant  $k_3$  under these conditions for the apparent rate law shown in eq 4.

$$-\frac{d[\text{I}]}{dt} = k_3[\text{OH}^-][\text{NO}][\text{I}] \quad (4)$$

**Mechanistic Schemes.** In the earlier communication,<sup>22</sup> we proposed on the basis of qualitative observations that **II** is formed by reaction of NO with a deprotonated amine of **I**, as illustrated in Scheme 1. This pathway is analogous to the inner-sphere mechanism for electron transfer between two metal centers mediated by a bridging ligand as first described by Henry Taube,<sup>36</sup> in this case NO being the reductant and Cu(II) the oxidant, with the coordinated amido anion as the bridging ligand. After electron transfer, demetallation of the

**Scheme 1.** Prospective Base-Dependent Mechanism for the Reductive Nitrosylation of **I**

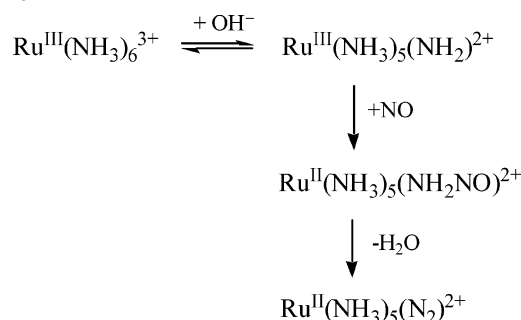
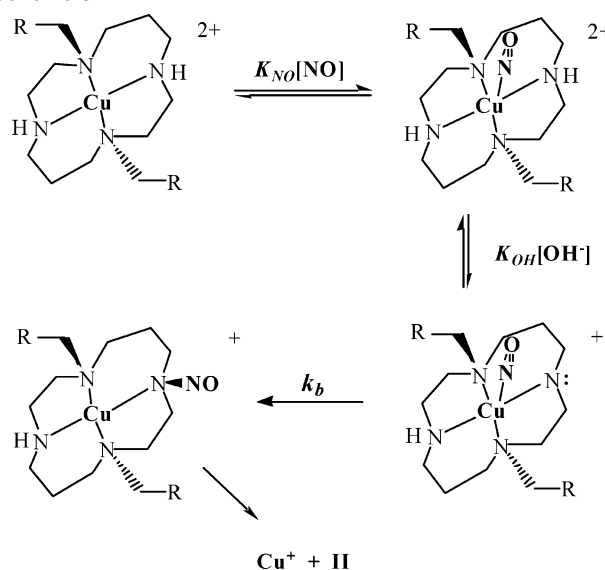
macrocyclic amine might be expected given the preference of Cu(I) for tetrahedral coordination and the lower ligand-donor strength of the nitrosoamine product.

If the reaction of NO with the deprotonated coordinated amine were rate limiting, the predicted rate law for Scheme 1 would be that described by eq 5, where  $[\text{I}]_{\text{tot}}$  is the sum of Cu(II) species. This would be consistent with the experimental behavior (eq 4, where  $k_3 = k_a K_{\text{OH}}$ ), if  $K_{\text{OH}}[\text{OH}^-] \ll 1$ . Under conditions where  $K_{\text{OH}}[\text{OH}^-]$  approaches 1, the plots of  $k_{\text{obs}}$  vs  $[\text{OH}^-]$  would show convex curvature and approach the limiting value  $k_a[\text{NO}]$  when  $K_{\text{OH}}[\text{OH}^-] \gg 1$ , but such leveling of  $k_{\text{obs}}$  was not obvious.<sup>37</sup>

$$-\frac{d[\text{I}]_{\text{tot}}}{dt} = k_{\text{obs}}[\text{I}]_{\text{tot}} = \frac{k_a K_{\text{OH}}[\text{OH}^-][\text{NO}][\text{I}]_{\text{tot}}}{K_{\text{OH}}[\text{OH}^-] + 1} \quad (5)$$

An apparent precedent of such a mechanism is found in the 1973 report by Armor et al.<sup>38</sup> that reaction of the ruthenium(III) complex  $\text{Ru}(\text{NH}_3)_6^{3+}$  with NO in alkaline solution leads to the formation of the Ru(II) dinitrogen complex  $\text{Ru}(\text{NH}_3)_5(\text{N}_2)^{2+}$ . This reaction is base catalyzed, and the Ru(III) complex is not substitution labile, thus the origin of the  $\text{N}_2$  ligand must be one of the amines. Scheme 2 displays a pathway involving NO nitrosation of a coordinated amide ligand with concomitant electron transfer to the Ru(III) and formation of a coordinated nitroso amine ligand. Subsequent dehydration would give the coordinated dinitrogen.

An alternative mechanism for the nitrosation of **I** that would involve initial nitric oxide coordination to the Cu(II) center ( $\text{Cu}^{\text{II}}(\text{NO}) \leftrightarrow \text{Cu}^{\text{I}}(\text{NO}^+)$ ) as first envisioned as a potential mechanism for NO sensing. This would be followed by amine deprotonation, then migration of  $\text{NO}^+$  to the

**Scheme 2****Scheme 3**

coordinated amide (giving the nitrosoamine) followed by dissociation of **II** from Cu(I), as depicted in Scheme 3. The predicted rate law would be eq 6. However, since saturation effects were not apparent for higher NO or base<sup>37</sup> concentrations,  $K_{\text{OH}}[\text{OH}^-]$  and  $K_{\text{NO}}[\text{NO}]$  must be small ( $\ll 1$ ) under the experimental conditions. In this case, eq 6 would simplify to  $k_{\text{obs}} = k_b K_{\text{OH}} K_{\text{NO}} [\text{OH}^-][\text{NO}]$ , consistent with the experimental observations (eq 4) and the rate law would be effectively indistinguishable from that for Scheme 1. However, one argument against Scheme 3 is the very weak bonding between the Cu(II) center and NO as predicted by DFT computations (see below); thus, the  $K_{\text{NO}}$  for formation of the hypothetical intermediate  $\text{Cu}^{\text{II}}(\text{DAC})(\text{NO})^{2+}$  is likely to be very small. A second issue is that there is no obvious reason why formation of the  $\text{Cu}^{\text{I}}(\text{NO})$  complex would enhance the acidity of the coordinated amine over that of **I** itself.

$$-\frac{d[\text{I}]_{\text{tot}}}{dt} = k_{\text{obs}}[\text{I}]_{\text{tot}} = \frac{k_b K_{\text{OH}} K_{\text{NO}} [\text{OH}^-][\text{NO}][\text{I}]_{\text{tot}}}{(K_{\text{OH}}[\text{OH}^-] + 1)(K_{\text{NO}}[\text{NO}] + 1)} \quad (6)$$

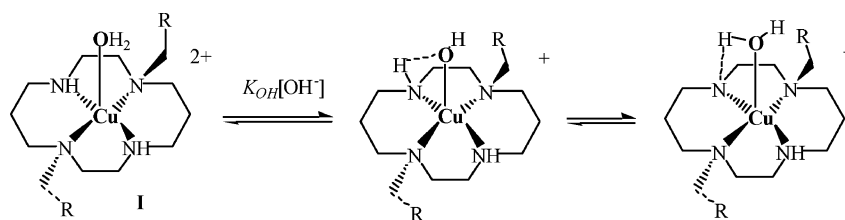
Although it was clear from the kinetics studies that complex formation with NO under the conditions explored must have a small  $K_{\text{NO}}$ , several attempts were made to use FTIR to probe the possible formation of a  $[\text{Cu}^{\text{II}}(\text{DAC})(\text{NO})]^{2+}$  via the reaction of **I** and NO in dry perdeuteroacetonitrile solution under which conditions deprotonation of the amine

(36) (a) The classic example of an inner-sphere electron transfer is the  $\text{Cr}^{2+}_{\text{aq}}$  reduction of  $\text{Co}(\text{NH}_3)_5\text{Cl}^{2+}$ , which results in Cl transfer to the chromium to give  $\text{Cr}(\text{H}_2\text{O})_5\text{Cl}^{2+}$  as one product.<sup>34</sup> (b) Taube, H.; Myers, H. *J. Am. Chem. Soc.* **1954**, *76*, 2103–2111.

(37) Although the plot of  $k_{\text{NO}}$  vs  $[\text{OH}^-]$  in Figure 5 (inset) might be viewed as having some curvature as predicted by eq. 5, we consider the deviation from linearity as within the experimental uncertainties of the kinetics data. Nonetheless, assuming the curvature to be valid and fitting the data to the function described by eq 5 gives a  $K_{\text{OH}}$  value of  $\sim 30 \text{ M}^{-1}$ .

(38) Pell, S. D.; Armor, J. N. *J. Am. Chem. Soc.* **1973**, *95*, 7625–7633.

Scheme 4



is unlikely. In a static experiment, the IR spectrum was recorded of a ambient temperature  $\text{CD}_3\text{CN}$  solution containing  $[\text{Cu}(\text{DAC})]\text{Br}_2$  (2.1 mM) equilibrated with NO (1 atm) in the absence of base and transferred to a  $\text{CaF}_2$  IR cell purged with NO. The second experiment used a custom-made rapid-flow IR apparatus in which  $\text{CD}_3\text{CN}$  solutions of **I** were rapidly mixed with NO solutions while acquiring the IR spectra. In neither experiment was a new IR absorption band observed over the frequency range ( $1600\text{--}1850\text{ cm}^{-1}$ ), typical for a coordinated nitrosyl group<sup>39</sup> under the conditions of the kinetics experiments.

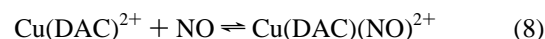
The present system can be compared to the earlier studies of NO oxidation by  $\text{CuL}_2(\text{H}_2\text{O})^{2+}$ , where L = phen (1,10-phenanthroline), dmp (eq 2), or dpp (2,9-diphenyl-1,10-phenanthroline) in various solutions.<sup>16</sup> The latter two  $\text{CuL}_2(\text{H}_2\text{O})^{2+}$  complexes are much stronger oxidants than most cupric complexes, owing to steric repulsion between the 2,9-substituents that favors the tetrahedral Cu(I). The kinetics of this reaction in water (eq 7) were followed by tracking the appearance of the strong metal-to-ligand charge transfer bands characteristic of the cuprous complexes  $\text{CuL}_2^+$ . The rates were first order in [NO], but there was no spectroscopic evidence of a  $\text{Cu}^{\text{II}}\text{--NO}$  intermediate. However, indirect evidence points toward a mechanism initiated by formation of such an intermediate. The  $\text{CuL}_2^{2+}$  oxidation of NO is faster when L is the less bulky dmp than when it is dpp, despite the latter complex being the stronger oxidant. Notably, for the  $\text{CuL}_2(\text{H}_2\text{O})^{2+}$  system the reaction with NO is somewhat inhibited by raising pH.



**DFT Calculations.** Computations at the BP/LACVP\* level were employed to examine likely intermediates in the reaction sequence. The calculated structure of the (gas phase)  $[\text{Cu}(\text{DAC})]^{2+}$  cation (see Supporting Information) was in reasonable agreement with the crystal structure (Figure 1) regarding the orientations of the pendant anthracenyl groups and bond lengths ( $\pm 0.05\text{ \AA}$ ) except for the Cu–N bonds, where the computed values are significantly larger than in the crystal structure. In the solid, the four nitrogens and the copper lie in a plane, while the optimized (gas phase) structure shows the tetradentate cyclam ligand slightly folded along one trans N–Cu–N axis. In both structures, the Cu–N bonds to the tertiary nitrogen atoms are somewhat longer than those to the secondary N's.

These computations also suggested that in aqueous solution the copper(II) would be lightly stabilized as an aquo complex

$\text{Cu}(\text{DAC})(\text{H}_2\text{O})^{2+}$  but that coordination of NO would be somewhat unfavorable (see Supporting Information). Thus, given the unfavorable entropic term implicit to the latter reaction (eq 8), the failure to observe a copper(II)-coordinated nitrosyl in the IR experiments is understandable, as is the failure to see saturation effects on the reaction kinetics at higher values of [NO].



On the other hand, coordination by hydroxide ion in the fifth position would appear to be very favorable even after solvation stabilization of the separated ions is taken into account.<sup>40</sup> According to the calculation, the coordinated  $\text{OH}^-$  would be stabilized by hydrogen bonding to an NH group. Furthermore, moving the bridging H to the hydroxyl to form the aquo-amido complex  $\text{Cu}(\text{DAC-H})(\text{H}_2\text{O})^+$  gives an optimized species a few kcal/mol lower energy than of the hydroxo complex. This suggests that a possible pathway for cyclam amine N–H deprotonation is an intramolecular proton transfer (Scheme 4).

The viability of the aquo-amido complex  $\text{Cu}(\text{DAC-H})(\text{H}_2\text{O})^+$  as an intermediate in the N-nitrosation reaction gains support from examining the DFT-computed singly occupied molecular orbital for  $\text{Cu}(\text{DAC-H})(\text{H}_2\text{O})^+$  (Figure 6). The SOMO includes significant contributions from Cu d orbitals (the largest from the  $d_{x^2-y^2}$  orbital) but also includes large contribution from the  $p_z$  orbital of the deprotonated amine nitrogen. Thus, the character of the SOMO would be consistent with that nitrogen being the site of a NO attack with simultaneous electron transfer to the metal to give a Cu(I) and the N-nitroso DAC.

## Summary

Coordination of DAC to copper(II) quenches all fluorescence from the pendant anthracene chromophores. Reaction with NO restores an anthracene-type emission, but the reaction leading to this change in photophysical properties is effectively irreversible. The change is not effected by NO coordination to the Cu(II) center but by nitrosation of a secondary cyclam amine ligand concomitant with reduction of Cu(II) to Cu(I). The new emission is attributed to the DAC–NO ligand, which dissociates from the cuprous ion, owing to the lower affinity between the **II** and  $\text{Cu}^+$ , perhaps because of the tendency of Cu(I) to favor tetrahedral coordination.

(39) Ford, P. C.; Lorkovic, I. M. *Chem. Rev.* **2002**, *102*, 993–1017.

(40) Palascak, M.; Shields, G. C. *J. Phys. Chem. A* **2004**, *108*, 3692–3694.



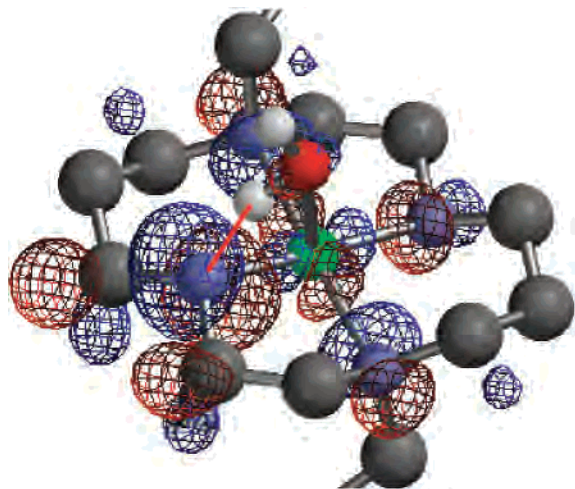


**Figure 6.** Graphical representation of the SOMO of [Cu(DAC-H)](H<sub>2</sub>O)<sup>+</sup> (H atoms, except for those on H<sub>2</sub>O and the anthracene groups are not shown).

Investigation of the kinetics in aqueous methanol solutions demonstrates the reaction to be first order in the concentrations of NO and of base. These data combined with insight gained from the DFT calculations are consistent with a reaction proceeding by attack of NO at an amine nitrogen that has been deprotonated by base, possibly via an intramolecular proton shift. In this model, electron transfer from the NO to the metal is accompanied by bond formation between the deprotonated cyclam nitrogen and the NO to form a nitroso-amine, effectively via an inner-sphere electron-transfer reaction.<sup>36</sup>

Reductions of metal centers by NO generally occur via formation of a metal nitrosyl species activated to attack by a solution nucleophile to give the nitroso-nucleophile product and the reduced metal center.<sup>6a</sup> There was little precedent for the mechanism described for the present reaction involving NO attack at a coordinated nucleophile and, until our preliminary report of the present study,<sup>22</sup> none for the formation of a stable nitroso amine product. Subsequent studies have demonstrated similar amine nitrosations coupled to the NO reductions of other polyamine complexes of copper(II),<sup>24</sup> and in the reaction of NO with Ni(III) methyl amine complex.<sup>41</sup> The reaction of NO with ruthenium(III) amines in alkaline media<sup>38</sup> would appear to be an historical precedent likely to be proceeding via a similar pathway as proposed by Scheme 2.

Nonetheless, such a mechanism for the nitrosation of coordinated ligands may have broader implications. For example, it was reported by Montfort et al.<sup>42</sup> that reaction of excess NO with bedbug nitrophorin (an NO carrier ferriheme protein in bedbug saliva) leads both to nitrosylation

and reduction of the heme iron and nitrosation of the proximal cysteine ligand (cys-60). Similarly, van Eldik et al.<sup>43</sup> described the reaction of a ferriheme thiolate model complex Fe<sup>III</sup>(P)(SR) with 2 equiv of NO to form the nitrosyl complex Fe<sup>III</sup>(P)(NO)(SR), then Fe<sup>II</sup>(P)(NO) plus RS-NO (eq 10). While it was proposed that such reactions might occur via



homolytic cleavage of the Fe–SR bond followed by trapping of the RS• radical by NO, these may instead proceed by NO attack at the coordinated thiolate ligand analogous to the reactions of Cu(DAC)<sup>2+</sup> described here. Notably, the inner-sphere mechanism involving NO attack at a coordinated ligand is the microscopic reverse of the decomposition of nitrosothiols catalyzed by copper(I),<sup>44</sup> which is likely to proceed via the initial coordination at the sulfur atom of RSNO followed by homolytic dissociation of the RS–NO bond. A similar example of the microscopic reverse of this ligand nitrosation mechanism would be the reaction of the ruthenium(II) octaethylporphyrin complex Ru<sup>II</sup>(OEP)(CO) with *S*-nitrosothiols to form the respective Ru<sup>II</sup>(OEP)(NO)-(thiolate) complex plus CO. Stopped-flow spectrophotometric studies showed this reaction to occur via an *S*-coordinated Ru<sup>II</sup>(OEP)(RSNO)(CO) intermediate.<sup>44</sup> The latter readily undergoes cleavage of the RS–NO bond to release NO, presumably to form Ru<sup>III</sup>(OEP)(RS)(CO) followed by NO replacement of coordinated CO to give the final product.

In these contexts, it appears that when an electron-rich ligand (such as an amine conjugate base or thiolate) is coordinated to a redox-active metal center, reductive nitrosylation by NO attack at that ligand, concomitant with electron transfer to the metal, is a viable mechanism for amine or thiol nitrosation. Such pathways should be among those considered in evaluating the reactivity of nitric oxide with biologically relevant metal centers.

**Acknowledgment.** These studies were supported by the National Science Foundation (CHE-0352650).

**Supporting Information Available:** Full citations for refs 11d and 19, figures showing the cell packing diagram for [Cu(DAC)]-(PF<sub>6</sub>)<sub>2</sub>, the ORTEP diagram of [Cu(DAC)](ClO<sub>4</sub>)<sub>2</sub>, the <sup>1</sup>H NMR spectrum recorded for DAC–NO, DFT structures calculated for Cu(DAC)(H<sub>2</sub>O)<sup>2+</sup> and Cu(DAC)(OH)<sup>+</sup>, sets of tables with crystal structure data for [Cu(DAC)](PF<sub>6</sub>)<sub>2</sub> and [Cu(DAC)](ClO<sub>4</sub>)<sub>2</sub>, the <sup>1</sup>H NMR resonances and assignments for DAC–NO, and the results of DFT calculations for Cu(DAC)<sup>2+</sup>, Cu(DAC)(H<sub>2</sub>O)<sup>2+</sup>, and Cu(DAC)(OH)<sup>+</sup>. This material is available free of charge via the Internet at <http://pubs.acs.org>.

IC7015929

(41) Shamir, D.; Zilbermann, I.; Maimon, E.; Cohen, H.; Meyerstein, D. *Inorg. Chem. Commun.* **2007**, *10*, 57–60.

(42) Weichsel, W.; Maes, E. M.; Andersen, J. F.; Valenzuela, J. G.; Shokhireva, T. K.; Walker, F. A.; Montfort, W. R. *Proc Natl. Acad. Sci. U.S.A.* **2005**, *102*, 594–599.

(43) Franke, A.; Stochel, G.; Suzuki, N.; Higuchi, T.; Okuzono, K.; van Eldik, R. *J. Am. Chem. Soc.* **2005**, *127*, 5360–5375.

(44) Dicks, A. P.; Swift, H. R.; Williams, D. L. H.; Butler, A. R.; Al-Sa'doni, H. H.; Cox, B. G. *J. Chem. Soc., Perkin Trans. 2* **1996**, 481–487.

(45) Andreasen, L. V.; Lorkovic, I. M.; Richter-Addo, G. B.; Ford, P. C. *Nitric Oxide* **2002**, *6*, 228–235.